Impurity modes in Frenkel exciton systems with dipolar interactions and cubic symmetry

ARTICLE *in* THE JOURNAL OF CHEMICAL PHYSICS · APRIL 2013

Impact Factor: 2.95 · DOI: 10.1063/1.4802057 · Source: PubMed

2 AUTHORS:

I. Avgin
Ege University
41 PUBLICATIONS **147** CITATIONS
SEE PROFILE

David Lawrence Huber
University of Wisconsin–Madison
93 PUBLICATIONS **788** CITATIONS
SEE PROFILE

Impurity modes in Frenkel exciton systems with dipolar interactions and cubic symmetry

I. Avgin and D. L. Huber

Citation: The Journal of Chemical Physics **138**, 164507 (2013); doi: 10.1063/1.4802057
View online: http://dx.doi.org/10.1063/1.4802057
View Table of Contents: http://scitation.aip.org/content/aip/journal/jcp/138/16?ver=pdfcov
Published by the AIP Publishing

Impurity modes in Frenkel exciton systems with dipolar interactions and cubic symmetry

I. Avgin[1,a)] and D. L. Huber[2,a),b)]
[1]*Department of Electrical and Electronic Engineering, Ege University, Bornova 35100, Izmir, Turkey*
[2]*Department of Physics, University of Wisconsin-Madison, Madison, Wisconsin 53706, USA*

(Received 4 February 2013; accepted 4 April 2013; published online 29 April 2013)

We introduce a continuum model for impurity modes of Frenkel excitons in fully occupied face-centered and body-centered cubic lattices with dipole-dipole interactions and parallel moments. In the absence of impurities, the model reproduces the small-k behavior found in numerical calculations of dipolar lattice sums. The exciton densities of states near the upper and lower band edges are calculated and compared with the corresponding results for a random array of dipoles. The Green function obtained with the continuum model, together with a spherical approximation to the Brillouin zone, is used to determine the conditions for the formation of a localized exciton mode associated with a shift in the transition energy of a single chromophore. The dependence of the local mode energy on the magnitude of the shift is ascertained. The formation of impurity bands at high concentrations of perturbed sites is investigated using the coherent potential approximation. The contribution of the impurity bands to the optical absorption is calculated in the coherent potential approximation. The locations of the optical absorption peaks of the dipolar system are shown to depend on the direction of propagation of the light relative to the dipolar axis, a property that is maintained in the presence of short-range interactions. © *2013 AIP Publishing LLC*. [http://dx.doi.org/10.1063/1.4802057]

I. INTRODUCTION

In an early paper on excitons,[1] Heller and Marcus developed a theory of Frenkel excitons in materials where the dominant interaction between chromophores was an electrostatic coupling involving the dipole moments associated with the optical transition between the ground and excited states. The analysis in Ref. 1 is based on a continuum approximation appropriate for a random array of dipoles as might be present in a diluted system. In this paper, we develop a continuum approximation for dipolar Frenkel excitons in fully occupied face-centered and body-centered cubic lattices. The continuum model is used in an investigation of localized Frenkel-exciton modes and impurity bands associated with chromophores perturbed by a shift in the optical transition energy. We calculate the optical absorption of the impurity bands and perturbed host bands and compare with the corresponding results for unperturbed arrays.

We assume that all of the transition dipole moments are equal and parallel to the z-axis so that the Hamiltonian of the unperturbed array is written

$$H = \mu^2 \sum_{i>j} (1 - 3z_{ij}^2/r_{ij}^2) r_{ij}^{-3}, \tag{1}$$

where the zero of energy is the optical transition energy of an unperturbed chromophore. Since the Fourier transforms of the lattice sums associated with the dipolar Hamiltonian of a spherical sample are independent of position when the radius of the sphere, R_S, satisfies the condition $kR_S \gg 10$ where k is the transform variable,[2] we postulate an array of N dipoles ($N \gg 1$) with periodic boundary conditions.

We start with a discussion of the continuum model introduced in Ref. 1. Since the authors do not provide the relevant details of their analysis, we outline the calculation of the exciton energy for the random array. Following Ref. 1, we approximate the array of randomly distributed chromophores as a uniaxial continuum with n_0 dipoles per unit volume. The exciton energy, $E(\vec{k})$, is then expressed as the integral

$$E(\vec{k}) = \mu^2 n_0 \int d\vec{r} \exp[i\vec{k} \cdot \vec{r}](1 - 3z^2/r^2)/r^3. \tag{2}$$

The next step is to make an expansion of the exponential in terms of spherical harmonics, Y_{lm}, and spherical Bessel functions j_l:

$$\exp[i\vec{k} \cdot \vec{r}] = 4\pi \sum_{l=0}^{\infty} \sum_{m=-l}^{l} i^l Y_{lm}(\theta_k, \phi_k) Y_{lm}^*(\theta, \phi), \tag{3}$$

where θ_k and ϕ_k denote the polar angles of the vector $\vec{k}$. Inserting Eq. (3) into Eq. (2) and making use of the fact that $(1 - 3z^2/r^2)$ is proportional to Y_{20}, together with the orthonormality of the spherical harmonics, we obtain the result

$$E(\vec{k}) = -4\pi\mu^2 n_0 (1 - 3\cos^2(\theta_K)) \int_R^{R_U} dr j_2(kr)/r, \tag{4}$$

where R denotes a lower cut-off. Following Ref. 1, in random arrays, we will take R to be the radius of a sphere of volume equal to the volume per dipole, $1/n_0$. In the continuum approximation, excluding the volume $1/n_0$ from the integral in Eq. (2) is equivalent to omitting the unphysical interaction of the dipole with itself. In cubic arrays, R will be determined

a)I. Avgin and D. L. Huber contributed equally to this work.
b)Author to whom correspondence should be addressed. Electronic mail: huber@src.wisc.edu

from the small-k expansion of the lattice dipolar sums (see below). The upper cutoff, R_U, is identified with a characteristic macroscopic dimension of the sample.

Making use of the properties of the spherical Bessel functions

$$j_2(x)/x = -(1/3)[dj_2(x)/dx - j_1(x)], \tag{5}$$

$$j_1(x) = -dj_0(x)/dx, \tag{6}$$

we can rewrite Eq. (4) as

$$E(\vec{k}) = \mu^2 n_0(3\cos^2(\theta_k) - 1)[b(kR) - b(kR_U)], \tag{7}$$

where

$$b(kR) = (4\pi/3)(j_0(kR) + j_2(kR)) \tag{8}$$

and

$$b(kR_U) = (4\pi/3)(j_0(kR_U) + j_2(kR_U)). \tag{9}$$

Note that while $E(0) = 0$, when $R_U \neq \infty$, $b(kR_U)$ can be neglected for finite k in a macroscopic sample so that we have

$$\begin{aligned} E(\vec{k}) &= \mu^2 n_0(3\cos^2(\theta_k) - 1)b(kR) \\ &= (4\pi/3)\mu^2 n_0(3\cos^2(\theta_k) - 1)[j_0(kR) + j_2(kR)] \\ &= 4\pi\mu^2 n_0(3\cos^2(\theta_k) - 1)(kR)^{-3} \\ &\quad \times [\sin(kR) - kR\cos(kR)], \end{aligned} \tag{10}$$

when $k \neq 0$. Equation (10) is the principal result of this section, expressing the exciton energy as a function of μ, n_0, R and the magnitude and polar angle (relative to the dipole alignment) of the exciton wave vector. It agrees with the result in Ref. 1, apart from the sign of the j_2 term which is given there as negative. In Fig. 1 we plot $b(kR)$ vs kR from 0 to 3.5. Note that when $kR \to 0$, the exciton energy becomes independent of the cut-off parameter. In this limit, the energy ranges between—$(4\pi/3)\mu^2 n_0$ and $(8\pi/3)\mu^2 n_0$, in agreement with the results of Refs. 1 and 2. In Secs. II–VI, it is understood that $k = 0$ refers to the limit $k = \varepsilon$, where ε denotes a small positive number.

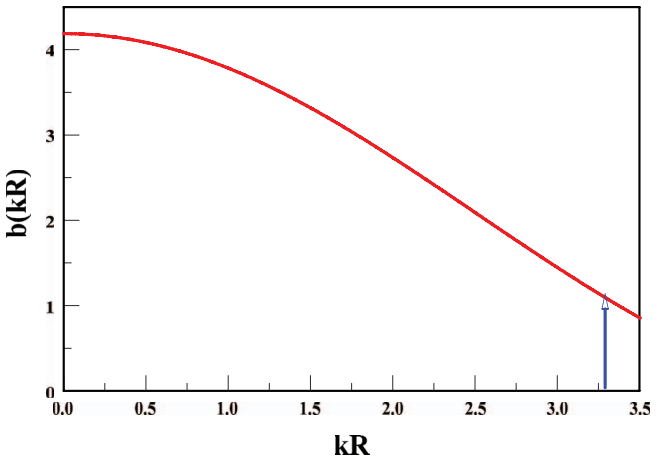

FIG. 1. $b(kR)$ vs kR where $b(kR) = (4\pi/3)[j_0(kR) + j_2(kR)] = 4\pi(kR)^{-3}[\sin(kR) - (kR)\cos(kR)]$. The numerical results are obtained from Eq. (10). The vertical arrow denotes the zone boundary in the spherical approximation to the Brillouin zones of face-centered and body-centered cubic lattices.

In Secs. II–VI, we extend the theory of the dipolar excitons to periodic arrays of chromophores on face-centered and body-centered cubic lattices. We develop a continuum model for the exciton energy that has the form of Eq. (10) but with a value for R appropriate for cubic lattices. With this expression we calculate the exciton density of states near the upper and lower band edges and compare our results with the corresponding results for the random distribution of dipoles. We use the results for the exciton energies to calculate the exciton Green function and obtain the condition for the formation of a localize exciton state induced by a shift in the optical transition energy of a single chromophore. The effects of finite concentrations of perturbed chromophores are calculated using the coherent potential approximation. At high impurity concentrations, split-off impurity bands are formed. The corresponding optical absorption shows both impurity band and perturbed host band absorption peaks.

II. CONTINUUM APPROXIMATION FOR CUBIC DIPOLAR ARRAYS

In this section, we develop a continuum approximation for the exciton energy in face-centered and body-centered cubic lattices. The approach is based on the observation that the corresponding expression for random arrays, Eq. (10), involves the cut-off parameter R. The critical step is to approximate the exciton energy in the cubic systems by Eq. (10) but with cubic cut-off factors, R (fcc) and R (bcc). The cubic cut-off parameters can be obtained from the quadratic terms in the expansion of the dipolar sums displayed in Ref. 2, Eq.(18′) and Table III. In the case of the fcc lattice, the quadratic term has the form

$$-0.473k^2a^2\left[3\left(k_z^2/k^2\right) - 1\right] \qquad \text{fcc},$$

while for the bcc lattice one has

$$-0.742k^2a^2\left[3\left(k_z^2/k^2\right) - 1\right] \qquad \text{bcc},$$

where a denotes the lattice parameter for the simple cubic unit cell containing four dipoles (fcc) or two dipoles (bcc). In carrying out the analysis we take the unit of energy to be $\mu^2 n_0$ and the unit of length to be $n_0^{-1/3}$. Rewriting the above expressions in these units, one obtains the fcc exciton energy to order k^2:

$$E(\vec{k}) = (4\pi/3)(3\cos^2(\theta_k) - 1)[1 - 0.0711k^2] \qquad \text{fcc}, \tag{11}$$

whereas the bcc exciton energy takes the form

$$E(\vec{k}) = (4\pi/3)(3\cos^2(\theta_k) - 1)[1 - 0.0703k^2] \qquad \text{bcc}. \tag{12}$$

To obtain the values of R for the two lattices we expand the right-hand side of Eq. (10) to order k^2

$$E(\vec{k}) = (4\pi/3)(3\cos^2(\theta_k) - 1)[1 - (1/10)k^2R^2]. \tag{13}$$

Comparing (11) and (12) with (13), we obtain

$$R(\text{fcc}) \approx 0.843, \tag{14}$$

for the fcc lattice and

$$R(\text{bcc}) \approx 0.839, \tag{15}$$

a nearly identical result, for the bcc lattice. These values are larger than the cut-off for the random array, which has the value $(3/4\pi)^{1/3} = 0.620$ in our units, so the self-interaction is omitted automatically. Since R (fcc) is close to R (bcc), we drop the distinction between the two lattices and refer to both of them as "cubic" with R (cubic) = 0.84.

In the continuum approach, the Brillouin zone associated with the cubic lattice is approximated by a sphere of volume equal to the volume of the zone. The radius of the sphere, k_0, is given by

$$k_0 = (6\pi^2 n_0)^{1/3}, \tag{16}$$

which becomes $k_0 = 3.90$ in the units of this paper.

III. EXCITON STATE DENSITIES IN CUBIC AND RANDOM DIPOLAR ARRAYS

In this section, we outline a calculation of the density of exciton states in unperturbed random and cubic polar arrays. In the continuum approximation, the density of states, denoted by $DOS(E)$, is defined by

$$DOS(E) = (1/8\pi^3)\int k^2 dk \int_0^{\pi} \sin(\theta_k) d\theta_k \times \int_0^{2\pi} d\phi_k \delta(E - E(\vec{k})), \tag{17}$$

where $E(\vec{k})$ is given by Eq. (10) with the appropriate value of R. Integrating over the angle ϕ_k the expression for the density of states becomes

$$DOS(E) = (1/2\pi^2)\int k^2 dk \int_0^1 dx \delta(E + b(kR) - 3x^2 b(kR)). \tag{18}$$

The integral over x is readily evaluated with the result

$$DOS(E) = (1/2\pi^2)\int_0^{k^*(E)} k^2 dk (6b(kR)x_0)^{-1}, \tag{19}$$

where x_0 is given by

$$x_0 = [(E + b(kR))/3b(kR)]^{1/2}. \tag{20}$$

The requirement that $0 \le x_0 \le 1$, imposes upper limits on the integral over k which we denote by $k^*{}_U(E)$ for the upper edge and $k^*{}_L(E)$ for the lower edge. The equation for $k^*{}_U(E)$ is

$$b(k_U^*(E)R) = 2E, \tag{21}$$

while $k^*{}_L(E)$ is the solution to the equation

$$b(k_L^*(E)R) = |E|. \tag{22}$$

In Figs. 2 and 3 we show the results for $DOS(E)$ near the upper and lower edges of the band for both random and cubic arrays. It is evident that while the densities of states for the four cases show quasi-linear behavior, the DOS associated with the lower edge is significantly larger than the DOS for the upper edge, and in both regions the density of states for the random array is greater than the density of states of the cubic arrays. The latter result can be traced to the inequality R (random) $< R$ (cubic).

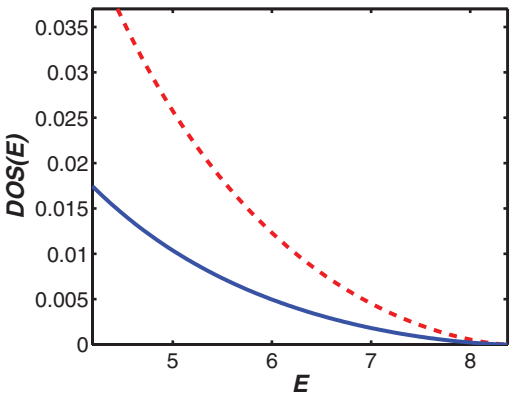

FIG. 2. Exciton densities of states, $DOS(E)$, near the upper band edge for a dipolar array in a cubic system ($R = 0.84$; solid curve) and a random system ($R = 0.62$; dashed curve). Note that in this figure, the range of E is such that the upper cut-off, $k^*{}_U(E)$, is less than the Brillouin zone cut-off k_0.

IV. LOCAL MODES AND IMPURITY BANDS IN PERTURBED DIPOLAR ARRAYS

In this section we investigate the local modes and impurity bands in fcc and bcc dipolar arrays where the optical transition energy of a single chromophore is shifted by an amount α. The condition for a local mode in a periodic array of dipoles involves the exciton Green function $G_0(E)$ defined by

$$G_0(E) = (1/N)\sum_{\vec{k}} [E - E(\vec{k})]^{-1}, \tag{23}$$

where the sum is over the N points of the Brillouin zone. The energy of a localized state outside the exciton band, E_{local}, is obtained from the equation

$$\alpha G_0(E_{local}) = 1, \tag{24}$$

first introduced by Koster and Slater in their analysis of localized states in a tight binding model of electronic structure.[3] A similar equation was also employed by Merrifield in an early investigation of localized states in Frenkel exciton systems,[4] with numerical results reported for one dimensional systems with nearest-neighbor interactions. Recently, the

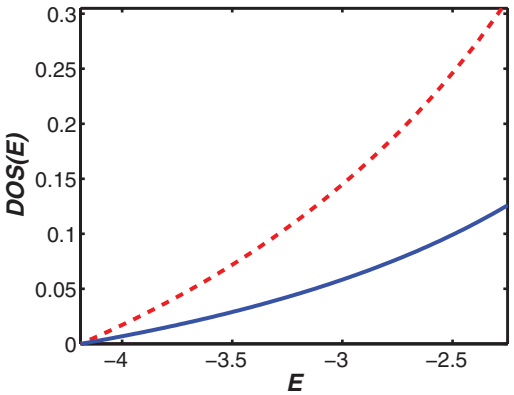

FIG. 3. Exciton densities of states, $DOS(E)$, near the lower band edge for a dipolar array in a cubic system ($R = 0.84$; solid curve) and a random system ($R = 0.62$; dashed curve). Note that in this figure, the range of E is such that the lower cut-off, $k^*{}_L(E)$, is less than the Brillouin zone cut-off k_0.

equation was utilized by the authors in an analysis of local modes associated with perturbed excitonic states of π-conjugated polymers.[5] In a related paper, the localized states in one-dimensional Frenkel exciton systems were investigated and a comparison was made between infinite-range and nearest-neighbor interactions.[6]

In the continuum approximation, the cubic Green function takes the form

$$G_0(E) = (1/2\pi^2)\int_0^{k_0} k^2 dk \int_0^1 dx[E - (3x^2 - 1)b(kR)]^{-1}. \quad (25)$$

The evaluation of the integral over x depends on whether the localized state is below or above the exciton band. For localized states above the band, we have

$$G_0(E) = (1/2\pi^2)\int_0^{k_0} k^2 dk[(3b(kR))(E + b(kR)]^{-1/2} \times \tanh^{-1}\left(\left[\frac{3b(kR)}{E + b(kR)}\right]^{1/2}\right), \quad (26)$$

while for localized states below the band, we find

$$G_0(E) = -(1/2\pi^2)\int_0^{k_0} k^2 dk[(3b(kR))(-E - b(kR)]^{-1/2} \times \tan^{-1}\left(\left[\frac{3b(kR)}{-E - b(kR)}\right]^{1/2}\right). \quad (27)$$

Note that $k_0R = 3.28$ for $R = 0.84$ so that $b(kR) > 0$ for $0 \le k \le k_0$ (see Fig. 1).

The variation of E_{local} with α is shown in Figs. 4 and 5. For localized states above the band $\alpha > 7.59$ while $\alpha < -3.06$ for localized states below the band. For comparison, had we taken $R = 0.62$, the value appropriate for a random array, we would have found that $\alpha > 6.97$ for localized states above the band and $\alpha < -2.41$ for localized states below the band. When $|\alpha| \gg 1$, E_{local} is approximately equal to α for positive and negative values of α. It can be shown that the 1/E asymptotic behavior of the Green function sets in at $E \approx 15$, when E is above the band, and at E ≈ -10, when E is below the band.

The presence of a finite concentration of impurities can give rise to impurity bands. To investigate the impurity bands

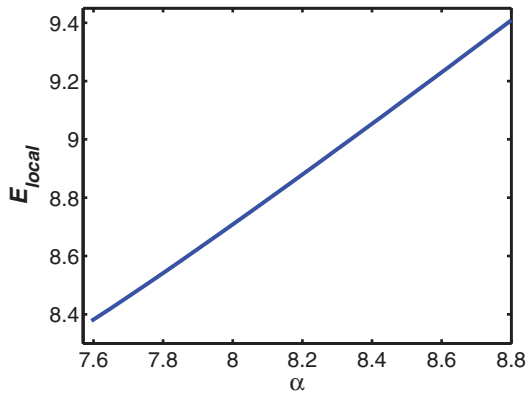

FIG. 4. Local mode energy, E_{local}, vs α for a cubic dipolar array, $\alpha > 0$; α denotes the shift in the optical transition energy of a single chromophore.

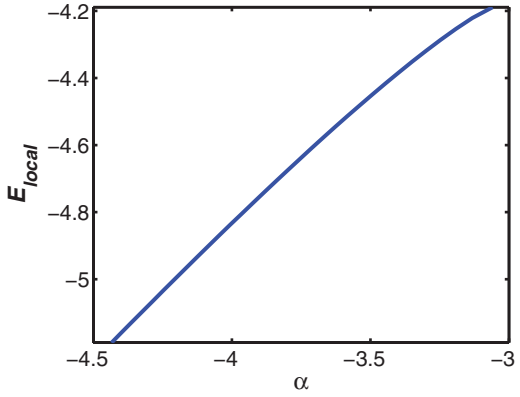

FIG. 5. Local mode energy, E_{local}, vs α for a cubic dipolar array, $\alpha < 0$; α denotes the shift in the optical transition energy of a single chromophore.

and their contribution to the optical absorption we make use of the coherent potential approximation (CPA).[7–9] When applied to a system where a fraction, c, of the chromophores have their transition energy shifted by α, the equation for the exciton Green function, $G_0^{\mathrm{CPA}}(E)$, from which one can calculate the density of states and the optical absorption, takes the form

$$G_0^{\mathrm{CPA}}(E) = (1/N)\sum_{\vec{k}}[E - \sigma(E) - E(\vec{k})]^{-1}, \quad (28)$$

where the coherent potential, $\sigma(E)$, is obtained from the self-consistent equation[9]

$$\sigma(E) = \alpha c/\left[1 - (\alpha - \sigma(E))G_0^{\mathrm{CPA}}(E)\right]. \quad (29)$$

In the CPA, the density of states is given by the imaginary part of $G_0^{\mathrm{CPA}}(E)$

$$DOS(E) = \pi^{-1}\left|\mathrm{Im}G_0^{\mathrm{CPA}}(E)\right|. \quad (30)$$

Results for the densities of states for $\alpha = 8$, and $c = 0.10$ and 0.25 are shown in Fig. 6. Note the presence of split-off impurity bands. With increasing impurity concentration, the impurity bands increase in spectral weight while their peak positions are approximately constant. The densities of states with $\alpha = -4$ and the same values of c are shown in Fig. 7. The spectral weights of the impurity bands again increase with increasing c, while the peak positions again are approximately constant. Unlike what was found for $\alpha = 8$, the impurity-host bandgap for $\alpha = -4$ shrinks with increasing impurity concentration.

V. OPTICAL ABSORPTION IN DIPOLAR ARRAYS

The CPA can also be used to obtain calculate the optical absorption.[9] In analyzing the absorption from the dipolar array, we assume that the incoming plane radiation is unpolarized. Since the transition dipole moments are along the z-axis, there is no absorption when the radiation is propagating in the z direction. For the pure system ($c = 0$), the optical absorption, $OA(E)$, when the direction of propagation makes an angle θ_k with the z-axis, takes the form

$$OA(E) = A\sin^2(\theta_k)\delta(E - (4\pi/3)[3\cos^2(\theta_k) - 1]), \quad (31)$$

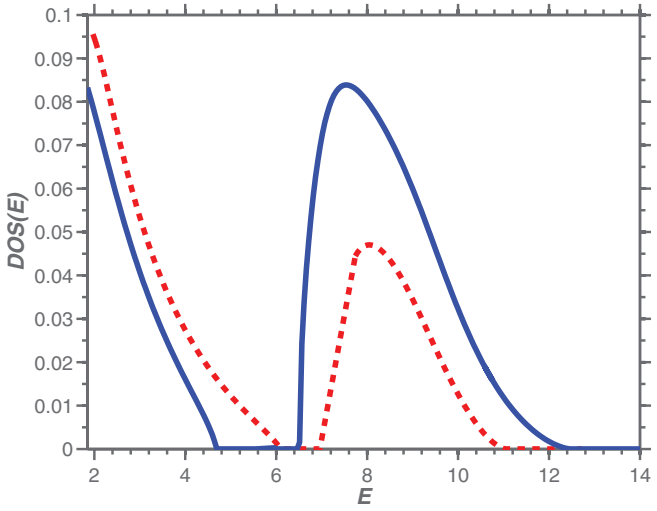

FIG. 6. Densities of states, $DOS(E)$, for $\alpha = 8$ and chromophore impurity concentrations $c = 0.10$ (dashed line) and 0.25 (solid line). α denotes the shift in the optical transition energy of the perturbed chromophores.

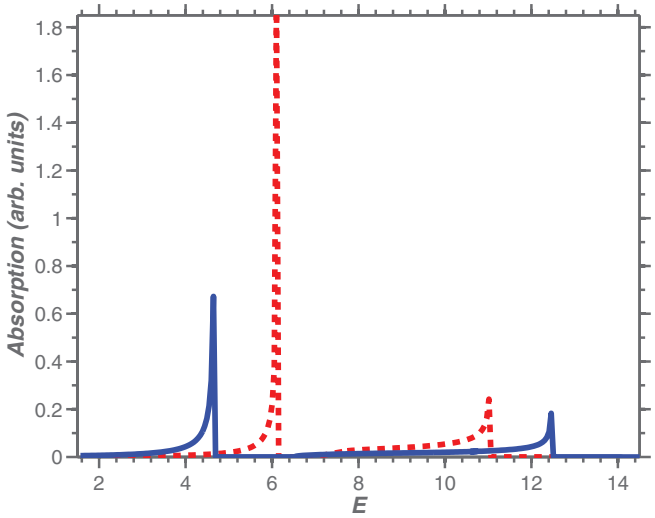

FIG. 8. Optical absorption for $\alpha = 8$ and impurity chromophore concentrations $c = 0.10$ (dashed line) and 0.25 (solid line). Unpolarized light; $\sin(\theta_k) \ll 1$. The factor $\sin^2(\theta_k)$ in Eq. (32) has been omitted to facilitate comparison with Fig. 9. The parameter α denotes the shift in the optical transition energy of the perturbed chromophores.

where A is a parameter whose comparatively slow variation with photon energy across the absorption band can be neglected. The angular factor $\sin^2(\theta_k)$ arises from the averaging of the square of the scalar product of the polarization vector and the dipole moment over a plane perpendicular to the direction of propagation.[10] The same factor also characterizes the angular dependence of the electromagnetic radiation from a dipole antenna. It should be noted that Eq. (31) applies to random as well as cubic arrays (see Eq. (10)).

In the presence of a finite concentration of impurities, the optical absorption in the CPA is expressed as[9]

$$OA(E) = A\sin^2(\theta_k)\pi^{-1}|\mathrm{Im}(\{E - \sigma(E) - (4\pi/3) \times [3\cos^2(\theta_k) - 1]\}^{-1})|. \quad (32)$$

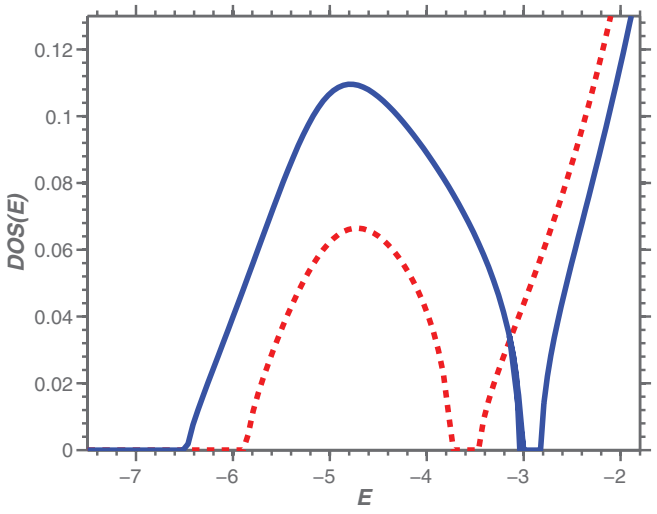

FIG. 7. Densities of states, $DOS(E)$, for $\alpha = -4$ and impurity chromophore concentrations $c = 0.10$ (dashed line) and 0.25 (solid line). α denotes the shift in the optical transition energy of the perturbed chromophores.

In Fig. 8, we show the absorption for unpolarized light propagating nearly parallel to the dipolar axis with the factor of $\sin^2(\theta_k)$ omitted for clarity. Results are shown for $\alpha = 8$, and $c = 0.10$ and 0.25. Note that the absorption peaks occur at the upper edges of the impurity bands, similar to what happens in the pure sample where the absorption peak for propagation nearly parallel to the dipole axis is at the upper band edge (see Eq. (31)). This feature reflects the fact that the impurity band wave functions are linear combinations of states near the upper band edge of the unperturbed host. While the impurity band edge shifts to higher energies with increasing impurity concentration, the absorption peaks associated with the host band shift to lower energies. This result is a consequence of the fact that the upper band-edge states of the perturbed host band are dominated by the contributions from states of the unperturbed system that are below the unperturbed band edge.

Results for $\alpha = -4$, and $c = 0.10$ and 0.25, with propagation perpendicular to the z-axis, are shown in Fig. 9. Note that absorption peaks occur at the lower edges of the impurity bands, similar to what happens in the pure sample when the absorption peak for propagation perpendicular to the dipole axis is at the lower band edge (see Eq. (31)). While the impurity band edge shifts to lower energies with increasing impurity concentration, the absorption peaks associated with the perturbed host band shift to higher energies. This result is a consequence of the fact that the lower band-edge states of the perturbed host band are dominated by the contributions from states of the unperturbed system that are above the unperturbed band edge. Unlike the situation with $\alpha = 8$, the oscillator strengths of the perturbed host bands for $c = 0.10$ and 0.25 are smaller than the oscillator strengths of the corresponding impurity bands. This feature may reflect the greater density of states near the lower band edge of the unperturbed array (see Fig. 3).

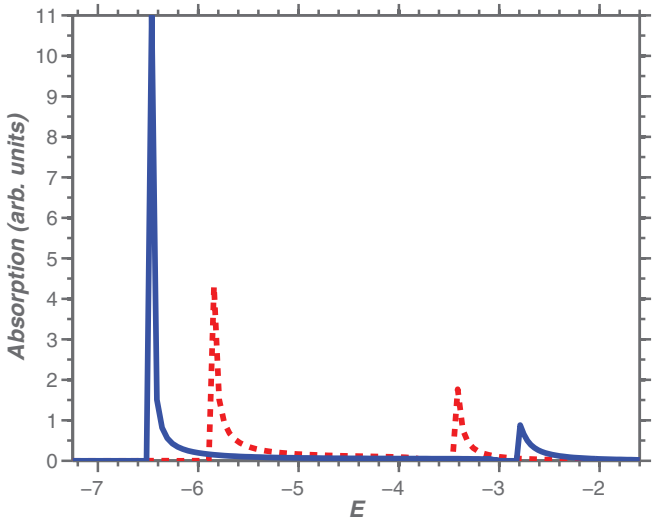

FIG. 9. Optical absorption for $\alpha = -4$ and chromophore impurity concentrations $c = 0.10$ (dashed line) and 0.25 (solid line). Unpolarized light, $\sin(\theta_k) = 1$. The parameter α denotes the shift in the optical transition energy of the perturbed chromophores.

VI. DISCUSSION

In Secs. II–V we have developed an approximate theory of dipolar Frenkel exciton systems having face-centered and body-centered cubic symmetry. After analyzing the properties of the cubic systems, we compared the density of exciton states of the cubic arrays with the corresponding density of states of a random array of dipoles. We also analyzed the effects of a shift in the transition energy of a single chromophore. It was shown that there are cut-offs such that localized exciton states in the upper and lower bands were present only when the shift exceeded the corresponding cut-off. This analysis was extended to a finite concentration of randomly distributed perturbed chromophores all having the same shift in transition energy. The densities of states of the impurity bands were calculated using the coherent potential approximation. The optical absorption of the ideal and perturbed arrays was also calculated with aid of the coherent potential approximation.

The continuum approximation utilized in the analysis of the cubic arrays reproduces the correct behavior in the exciton dispersion of the unperturbed array to order k^2. As a consequence it gives accurate results for the density of states near the band edges (Figs. 2 and 3). Our extension of the continuum dispersion to larger k (done in the spirit of the Debye model for phonons), along with a spherical approximation to the Brillouin zone, makes it possible to reduce the calculation of G_0 to the numerical evaluation of a one-dimensional integral over a finite range. Although the continuum approach is a severe approximation, it is made to the integrand in the integral for G_0 and yields the correct limiting behavior for large $|E|$.

Since the dipole-dipole interaction is relatively weak, even in dense arrays, the question arises as to whether the effects we have investigated can be observed in materials where there are strong short-range interactions in addition to a coupling between parallel transition dipoles. The answer to this question is a qualified "yes." The angular dependence of the optical absorption peaks displayed in Eqs. (31) and (32) depends on the angle between the direction of the propagation of the light and the dipolar axis. At optical wavelengths, only the isotropic long wavelength limit of the Fourier transform of the short-range interactions appears in the exciton absorption spectrum. Thus the unique signature of the dipolar interaction, the dependence of the location of the absorption peaks on the direction of propagation of the light, is retained. It should be noted that dipolar effects of the type studied here can also appear in magnetic dipole spectra, although the oscillator strengths of the transitions are much smaller.

ACKNOWLEDGMENTS

I. Avgin would like to thank the Scientific and Technological Research Council of Turkey (TUBITAK) for their partial support.

[1]W. R. Heller and A. Marcus, Phys. Rev. **84**, 809 (1951).
[2]M. H. Cohen and F. Keffer, Phys. Rev. **99**, 1128 (1955); Phys. Rev. B **10**, 787 (1974).
[3]G. F. Coster and J. C. Slater, Phys. Rev. **95**, 1167 (1954); **96**, 1208 (1954).
[4]R. E. Merrifield, J. Chem. Phys. **38**, 920 (1963).
[5]I. Avgin, M. Winokur, and D. L. Huber, J. Lumin. **125**, 108 (2007).
[6]I. Avgin and D. L. Huber, J. Phys. Chem. B **113**, 14112 (2009).
[7]P. Soven, Phys. Rev. **156**, 809 (1967).
[8]D. W. Taylor, Phys. Rev. **156**, 1017 (1967).
[9]F. Yonezawa and K. Morigaki, Prog. Theor. Phys. Suppl. **53**, 1 (1973).
[10]V. M. Agranovich, *Excitations in Organic Solids* (Oxford University Press, New York, 2009), Chap. 4.